Available online at www.sciencedirect.com
ScienceDirect
Bioorganic & Medicinal Chemistry 16 (2008) 3694–3703
Bioorganic & Medicinal Chemistry

Methoxylation of 3′,4′-aromatic side chains improves P-glycoprotein inhibitory and multidrug resistance reversal activities of 7,8-pyranocoumarin against cancer cells

Wang-Fun Fong,[a,*] Xiao-Ling Shen,[b] Christoph Globisch,[c] Michael Wiese,[c] Guang-Ying Chen,[d] Guo-Yuan Zhu,[a] Zhi-Ling Yu,[a] Anfernee Kai-Wing Tse[a] and Ying-Jie Hu[e]

[a]*Research & Development Division, School of Chinese Medicine, Hong Kong Baptist University, Kowloon Tong, Hong Kong SAR, China*
[b]*Department of Biology and Chemistry, City University of Hong Kong, Hong Kong SAR, China*
[c]*Institute of Pharmacy, University of Bonn, An der Immennburg 4, 53121 Bonn, Germany*
[d]*Department of Chemistry, Hainan Normal University, Haikou, China*
[e]*Research Group of Pharmaceutical Sciences, Tropical Medicine Institute, Guangzhou University of Chinese Medicine, Guangzhou, China*

Received 6 December 2007; revised 26 January 2008; accepted 2 February 2008
Available online 13 February 2008

Abstract—The overexpression of P-glycoprotein (Pgp), an ATP-driven membrane exporter of hydrophobic xenobiotics, is one of the major causes of multidrug resistance (MDR) in cancer cells. Through extensive screening we have found that the extracts of *Peucedanum praeruptorum* Dunn. and one of the major components (±)-praeruptorin A (PA) may reverse Pgp-mediated multidrug resistance. Studies on novel PA derivatives have shown that (±)-3′-*O*,4′-*O*-dicinnamoyl-*cis*-khellactone (DCK) is more active than PA or verapamil and is a non-competitive inhibitor of Pgp. Here, we report that methoxylation of the cinnamoyl groups on DCK may further enhance its bioactivity. The structure–activity relationship is demonstrated by comparing two new pyranocoumarins (±)-3′-*O*,4′-*O*-bis(3,4-dimethoxycinnamoyl)-*cis*-khellactone (DMDCK) and (±)-3′-*O*,4′-*O*-bis(4-methoxycinnamoyl)-*cis*-khellactone (MMDCK). While the co-existence of 3- and 4-methoxy groups on cinnamoyl remarkably enhanced the Pgp-inhibitory activity, the lone existence of the 4-methoxy group on cinnamoyl reduced the activity. Contrary to DCK, DMDCK promoted the binding of UIC2 antibody to Pgp which signifies a conformational change of Pgp similar to that induced by transport substrates. While DCK moderately stimulated the basal Pgp-ATPase activity, DMDCK inhibited the activity. A pharmacophore search with verapamil-based template revealed that four functional groups of DMDCK could be simultaneously involved in interaction with Pgp whereas for DCK or MMDCK only three groups were involved. It is speculated that the additional 3-methoxy group on cinnamoyl allows DMDCK to interact more efficiently with Pgp substrate site(s). If DMDCK was tightly bind to Pgp substrate site(s) the complexes could be inactive with regard to transportation and ATP hydrolysis could also be inhibited.

1. Introduction

Multidrug resistance (MDR) of cancer cells is often an obstacle for successful chemotherapy and one of its better understood causes is the overexpression of P-glycoprotein (Pgp), a 170-kDa membrane ATP-driven drug exporter encoded by MDR1 gene. Pgp actively extrudes a spectrum of hydrophobic xenobiotics, including a number of anticancer drugs.[1–3] Pgp inhibitors may be able to reverse Pgp-mediated MDR (Pgp-MDR) and many are competitive inhibitors.[4–6] Other effective Pgp-MDR reversal agents are non-competitive inhibitors such as XR9576 and *cis*-(*Z*)-flupentixol that interact with the substrate site(s) but are not transported.[7–10] Still others such as curcumin or (±)- praeruptorin A may modulate Pgp expression.[11,12]

The three-dimensional structure of Pgp has not been determined but based on biochemical studies it is

Keywords: P-glycoprotein; Multidrug resistance; (±)-3′-*O*,4′-*O*-dicinnamoyl-*cis*-khellactone; (±)-3′-*O*,4′-*O*-bis(3,4-dimethoxycinnamoyl)-*cis*-khellactone.
* Corresponding author. Tel.: +852 34112928; fax: +852 34112902; e-mail: wffong@hkbu.edu.hk

0968-0896/$ - see front matter © 2008 Elsevier Ltd. All rights reserved.
doi:10.1016/j.bmc.2008.02.029

speculated that Pgp has multiple substrate-binding sites and also a allosteric regulatory site.[13] Several pharmacophore models have been developed based on three-dimensional quantitative structure–activity relationship studies (QSAR) on highly active Pgp substrates or inhibitors. For these pharmacophore models locations and spatial relationship of various chemical groups including aromatic rings, hydrogen bond (HB) acceptors (O or N atom) and HB donors (OH or NH group) have been determined.[14–18]

We have shown that (±)-praeruptorin A (PA), a naturally occurring 7,8-pyranocoumarin abundantly found in *Peucedanum praeruptorum* Dunn., is able to suppress Pgp expression and reverse Pgp-MDR in KB V1 cells.[12] In an attempt to develop new and more potent Pgp inhibitors we synthesized a number of PA derivatives and studied their structure–activity relationship. The first group of new derivatives were obtained by replacing the two aliphatic acyls at C-3′-O and C-4′-O sites of 7,8-pyranocoumarin with various aliphatic or aromatic acyls. We have previously reported that one of these new semi-synthetic compounds, (±)-3′-*O*,4′-*O*-dicinnamoyl-*cis*-khellactone (DCK), is more potent than PA or verapamil in reversing Pgp-MDR.[19] Interestingly unlike PA that suppresses Pgp expression DCK does not but instead binds directly to Pgp. In this report, we give a detailed account on structure–activity relationship of two new methoxylated compounds (±)-3′-*O*,4′-*O*-bis(3,4-dimethoxycinnamoyl)-*cis*-khellactone (DMDCK) and (±)-3′-*O*,4′-*O*-bis(4-methoxycinnamoyl)-*cis*-khellactone (MMDCK) (Fig. 1).

2. Results and discussion

2.1. Preparation of DMDCK and MMDCK

DMDCK and MMDCK (Fig. 1) were prepared by the same chemical reactions as used in DCK synthesis except that cinnamic acid was replaced by 3,4-dimethoxycinnamic acid or 4-methoxycinnamic acid, respectively.[19] Both DMDCK and MMDCK are new compounds with zero specific optical rotations. Together with MS and NMR data, their structures were determined as shown in Figure 1.

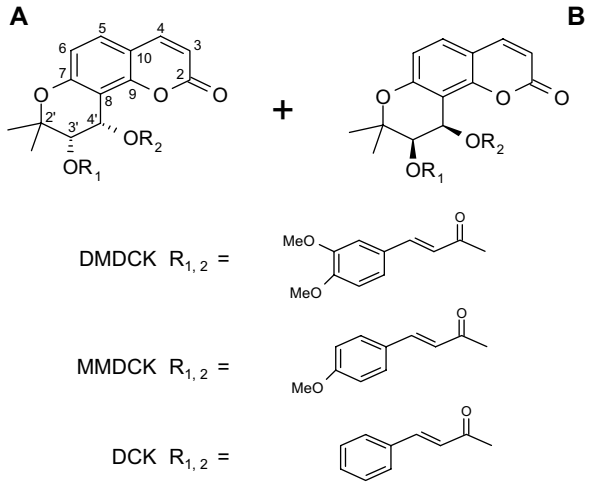

Figure 1. Structures of DMDCK and MMDCK. DMDCK and MMDCK are racemates consisting equal amount of enantiomers described as A and B, respectively.

2.2. Pgp-MDR reversal activity of DMDCK and MMDCK

It has been shown that in comparison to drug sensitive HepG2 and K562 cells, Pgp overexpressing HepG2/Dox and K562/Dox cells are highly resistant to vinblastine, doxorubicin, puromycin, and paclitaxel that are all Pgp substrates.[19] Compared to drug sensitive KB-3-1 cells, Pgp overexpressing KB V1 cells were 9271, 178, 378, and 400 times more resistant to vinblastine, doxorubicin, puromycin, and paclitaxel, respectively (Table 1). MDR reversal activities of various chemicals were evaluated in Pgp-MDR cells treated with various doses of a cancer drug and results are expressed as changes in IC_{50} (the concentration inhibiting cell growth by 50%). In HepG2/Dox cells, IC_{50} values of vinblastine, doxorubicin, puromycin, and paclitaxel were reduced by 4 μM of DMDCK by 110-, 167-, 123-, and 138-fold, respectively (Table 2). Corresponding decreases by DCK treatment were 28-, 21-, 18-, and 24-fold, respectively.[19] DMDCK showed similar MDR reversing effects on K562/Dox and KB-V1 cells (Table 3). The decreases in IC_{50} values were not observed in drug sensitive HepG2 cells (Table 2), implying that DMDCK and MMDCK mainly acted on the overexpressed Pgp that distinguishes Pgp-MDR cells from drug sensitive cells. MMDCK also significantly reversed drug resistance in HepG2/Dox and K562/Dox cells but was less effective than DCK (Tables 2 and 3).

2.3. DMDCK was more effective than DCK in inhibiting Pgp substrate efflux

Next we investigated the effect of DMDCK and DCK on drug efflux in Pgp-MDR HepG2/Dox and K562/Dox cells. Consistent with their effects on MDR reversal, DMDCK was far more effective than DCK in inhibiting rhodamine 123 (Rh-123, a Pgp substrate) efflux from both MDR cell lines (Fig. 2). In the presence of 10 μM DMDCK, the cellular fluorescence of Rh-123 increased by 200% and 480% in K562/Dox and HepG2/Dox cells, respectively. In comparison 10 μM DCK increased cellular fluorescence by only 20% and 50% in K562/Dox and HepG2/Dox cells, respectively. It has been proposed that Pgp has multiple transport sites and Rh-123 is transported by the R-site.[13] Another transport site is known as the H-site that is particularly effective in the transportation of Hoechst 33342.[13,20] Both DMDCK and DCK inhibited Hoechst 33342 efflux from MDR cells in a dose-dependent manner and at their respective optimum dose 5 μM DMDCK increased cellular Hoechst 33342 fluorescence by about 200% and DCK at 10 μM by about 100% (Fig. 3).

2.4. DMDCK did not affect Pgp expression level in MDR cells

As mentioned above PA mainly affects cellular Pgp activity by suppressing the expression of the protein.[12]

Table 1. Growth inhibitory effect of anticancer drugs, DMDCK, and MMDCK (IC_{50}, μM)

	Vinblastine	Doxorubicin	Puromycin	Paclitaxel	DMDCK	MMDCK
KB-3-1[a]	0.11 ± 0.01 ($\times10^{-3}$)	0.18 ± 0.04	0.21 ± 0.05	0.002 ± 0.001	61.68 ± 0.63	—
KB V1[a]	1.04 ± 0.34	31.98 ± 2.74	79.30 ± 8.81	8.00 ± 1. 48	32.30 ± 3.25	—
RR[c]	9271	178	378	400		
HepG2[a]	0.07 ± 0.03 ($\times10^{-3}$)	0.11 ± 0.04	0.23 ± 0.04	0.007 ± 0.003	54.70 ± 3.02	55.20 ± 5.52
HepG2/Dox[a]	0.44 ± 0.09	36.74 ± 1.88	83.93 ± 17.61	4.15 ± 0. 11	76.33 ± 2.22	72.62 ± 0.30
RR[c]	5946	334	364	592		
K562[b]	0.88 ± 0.25 ($\times10^{-3}$)	0.24 ± 0.08	0.22 ± 0.09	0.60 ± 0.23 ($\times10^{-3}$)	54.43 ± 4.24	67.59 ± 7.08
K562/Dox[b]	0.17 ± 0.07	24.14 ± 3.44	26.83 ± 2.50	4. 14 ± 0.23	70.01 ± 3.10	81.02 ± 17.07
RR[c]	193	101	122	6900		

Cells were exposed to drugs for 72 h and IC_{50} (μM drug concentration inhibiting 50% of cell growth) was determined and presented as means ± SD of three experiments.

[a] IC_{50} was determined by MTT assay.

[b] IC_{50} was determined by SRB assay.

[c] RR = resistant ratio = $IC_{50\ (MDR\ cell)}/IC_{50\ (parental\ cell)}$.

Table 2. Effects of MMDCK and DMDCK on drug sensitivity of HepG2 and HepG2/Dox cells

	HepG2/Dox		HepG2	
	IC_{50} (μM)	Folds increased in drug sensitivity[a]	IC_{50} (μM)	Folds increased in drug sensitivity[a]
Vinblastine	0.44 ± 0.09		0.07 ± 0.03 (nM)	
With MMDCK	0.09 ± 0.04	4.9	0.06 ± 0.04 (nM)	1.1
With DMDCK	0.004 ± 0.002	110.0	0.08 ± 0.02 (nM)	0.9
With DCK[b]		28.2		1.1
Doxorubicin	36.74 ± 1.88		0.11 ± 0.04	
With MMDCK	1.98 ± 0.66	18.6	0.15 ± 0.03	0.7
With DMDCK	0.22 ± 0.02	167.0	0.15 ± 0.04	0.7
With DCK[b]		20.8		1.1
Puromycin	83.93 ± 17.61		0.23 ± 0.04	
With MMDCK	7.59 ± 2.13	11.0	0.20 ± 0.03	1.1
With DMDCK	0.68 ± 0.29	123.4	0.17 ± 0.07	1.3
With DCK[b]		17.6		1.2
Paclitaxel	4.15 ± 0.11		0.007 ± 0.003	
With MMDCK	0.53 ± 0.16	7.8	0.006 ± 0.001	1.1
With DMDCK	0.03 ± 0.01	138.3	0.007 ± 0.001	1.0
With DCK[b]		23.5		0.6

HepG2 and HepG2/Dox cells were exposed to anticancer drugs in the presence of 4 μM DMDCK or MMDCK for 72 h and IC_{50} (μM drug concentration inhibiting 50% growth) was determined by SRB assay. Values are means ± SD of three experiments.

[a] Folds increased in drug sensitivity = (IC_{50} of control)/(IC_{50} in the presence of modulator).

[b] Data are from Ref. 19.

Effect of DMDCK on Pgp expression level was investigated in Pgp overexpressing HepG2/Dox, K562/Dox, and KB V1 cells. As shown in Figure 4, treatments with 4, 8, or 20 μM of DMDCK for 72 h did not affect Pgp expression.

2.5. DMDCK increased Pgp reactivity to UIC2

The monoclonal antibody UIC2 preferentially recognizes Pgp when its substrate sites are being occupied by substrates or competitive inhibitors.[21,22] On the contrary allosteric inhibitors may decrease UIC2 reactivity. DCK decreased UIC2 binding to HepG2/Dox cells[19] but DMDCK increased UIC2 labeling of HepG2/Dox cells (Fig. 5). These observations imply that DMDCK perhaps was able to interact with the substrate site(s) of Pgp.

2.6. Effect of DMDCK on Pgp-ATPase activity

Pgp-mediated drug transport is tightly coupled to ATP hydrolysis that can be measured in the presence of substrates. Verapamil and progesterone are two standard Pgp transport substrates that stimulate Pgp-ATPase activity according to Michealis–Menten kinetics (Fig. 7). Pgp-ATPase activity was studied in Pgp-rich membrane fractions prepared from Pgp overexpressing cells while suppressing the activities of other major membrane ATPases. DCK slightly stimulates basal Pgp-ATPase activity but inhibits substrate-stimulated ATP hydrolysis in a non-competitive manner[19] suggesting that although DCK may have some substrate-like property but overall DCK impedes the transport activity. Unlike DCK, DMDCK inhibited the basal Pgp-ATPase activity (Fig. 6) as well as substrate-stimulated

Table 3. Effects of MMDCK and DMDCK on drug sensitivity of K562/Dox and KB V1 cells

	K562/Dox[a]		KB V1[b]	
	IC_{50} (μM)	Sensitivity increased[a]	IC_{50} (μM)	Sensitivity increased[a]
Vinblastine	0.17 ± 0.07		1.04 ± 0.34	
With DMDCK	0.001 ± 0.001	121.0	0.004 ± 0.002	260.0
With MMDCK	0.019 ± 0.013	8.9	ND	
With DCK[c]		28.6	ND	
Doxorubicin	24.14 ± 3.44		31.98 ± 2.74	
With DMDCK	0.60 ± 0.19	40.2	0.97 ± 0.44	33.0
With MMDCK	2.95 ± 1.12	8.2	ND	
With DCK[c]		15.0	ND	
Puromycin	26.83 ± 2.50		79.30 ± 8.81	
With DMDCK	0.74 ± 0.20	36.2	0.68 ± 0.05	116.6
With MMDCK	3.27 ± 0.97	8.2	ND	
With DCK[c]		11.3		
Paclitaxel	4.14 ± 0.23		8.00 ± 1.48	
With DMDCK	0.02 ± 0.01	207.0	0.02 ± 0.01	400.0
With MMDCK	0.27 ± 0.13	15.3	ND	
With DCK[c]		108.3	ND	

Cells were exposed to anticancer drugs in the presence of 4 μM DMDCK or MMDCK for 72 h. Values are means ± SD of three experiments. ND, not determined.

[a] IC_{50} was determined by MTT assay.

[b] IC_{50} was determined by SRB assay.

[c] Data are from Ref. 19.

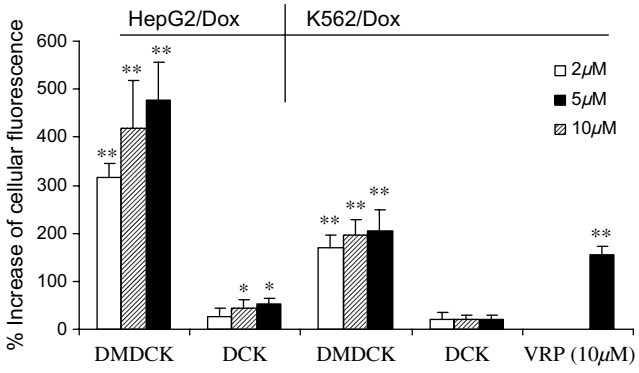

Figure 2. Inhibitory effect of DMDCK and DCK on Rh-123 efflux in K562/Dox cells or HepG2/Dox cells. Cells were treated with 5 μg/mL Rh-123 for 1 h followed by an additional hour of incubation with 0, 2, 5, or 10 μM of DMDCK, DCK, or 10 μM verapamil (VRP) in Rh-123 free medium. Cellular fluorescence was monitored by flow cytometry. Increase of cellular fluorescence is shown in percentage. Results are means of three experiments. Significantly different at $^{*}P < 0.05$ and $^{**}P < 0.01$ levels as compared with based line control.

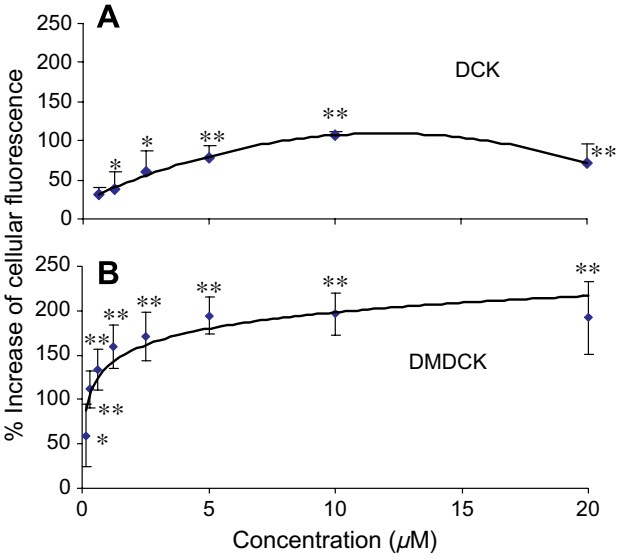

Figure 3. Inhibitory effect of DMDCK and DCK on Hoechst 33342 efflux in HepG2/Dox cells. Cells in 96-well plates were treated with 20 μg/mL Hoechst for 1 h followed by an additional hour of incubation with various concentrations of DMDCK or DCK in Hoechst 33342 free medium. Increase of cellular fluorescence is shown in percentage. Results are mean values of three experiments. Significantly different at $^{*}P < 0.05$ and $^{**}P < 0.01$ compared with based line control. Basal activity was subtracted as background.

ATP hydrolysis (Fig. 7) indicating that DMDCK is not a transport substrate of Pgp but is an effective inhibitor of Pgp-mediated transport. In the presence of 1 μM DMDCK both verapamil- and progesterone-stimulated ATP hydrolysis were inhibited with reduced V_{max} and relatively steady K_m, suggesting a non-competitive mode of inhibition.

2.7. Structure–activity relationship

Summarizing our observations first although DMDCK, MMDCK, and DCK share the same core structure, DMDCK, bearing two 3,4-dimethoxycinnamoyl groups, was the most effective Pgp inhibitor. With two 4-methoxycinnamoyl groups MMDCK was the least active. Second, DMDCK increased UIC2 monoclonal antibody binding to Pgp but effectively inhibited Pgp-catalyzed ATP hydrolysis; on the other hand, DCK decreased UIC2 binding and slightly increased ATP hydrolysis. Thus, it can be speculated that DMDCK

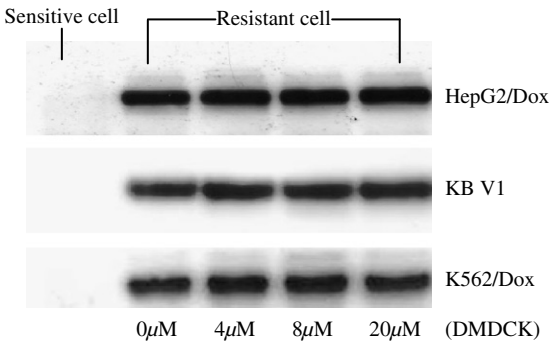

Figure 4. Effect of DMDCK on Pgp expression in Pgp-MDR cells. HepG2/Dox, K562/Dox or KB-V1 cells were incubated with or without 0, 4, 8, or 20 μM DMDCK for 72 h. Cells were lysed, centrifuged and supernatant samples each containing 50 μg of total cellular protein were separated by 10% SDS–PAGE. Pgp was detected by specific antibody. Samples in lane 1 were from untreated drug sensitive HepG2, K562, and KB-3-1 cells.

had a better fit to substrate site(s) but by so doing it inhibited the subsequent transportation processes whereas DCK fit loosely to substrate site(s) but could be transported.

Verapamil-based pharmacophore model for Pgp substrates or inhibitors proposed by Pajeva et al. involves two essential hydrophobic planes, three optional HB acceptor points and one optional HB donor point with spatial arrangement (Fig. 8).[17] According to this model, the more active the drug, either more pharmacophore points are simultaneously occupied, or the number of possible binding modes increases. Different drugs can interact with different receptor points on Pgp in different binding modes. In this study, pharmacophore search for DMDCK, MMDCK, and DCK with verapamil-based pharmacophore template was performed. Results showed that all three compounds matched the model well (Table 4). Both stereoisomers of DMDCK had four functional groups (two hydrophobic points and two HB accepter points) simultaneously involved in interaction with Pgp, implying a higher binding affinity and Pgp modulating activity. MMDCK has only one conformation of stereoisomer A matching the pharmacophore with four functional groups. DCK had three groups involved simultaneously, suggesting a relatively lower affinity and modulating activity. It is the 3-methoxy but not the 4-methoxy on cinnamoyl that is in the right position and orientation to interact with Pgp as a HB accepter. Results of the pharmacophore search provide an explanation on structural bases for MDR reversing activity of the three compounds.

3. Conclusion

Neither DMDCK nor DCK affects Pgp expression level but instead they directly interact with Pgp. Methoxy groups on aromatic rings can significantly alter the mode of interaction between Pgp and pyranocoumarins and affect Pgp-MDR reversing activity. The existence of 3,4-dimethoxy substructure on cinnamoyl significantly

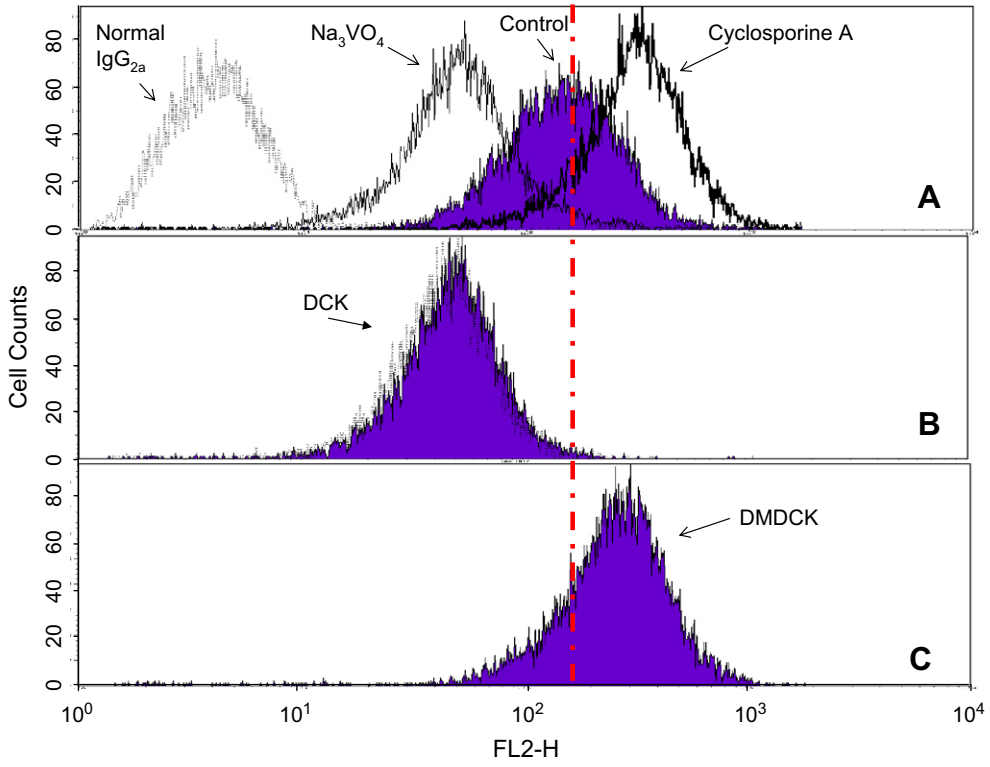

Figure 5. Effect of DMDCK on Pgp-UIC2 reactivity. HepG2/Dox cells were incubated with UIC2 monoclonal antibody at 37 °C, in the presence or absence (control) of 1 mM Na_3VO_4, 5 μM cyclosporine A (A), 5 μM DCK (B), or 5 μM DMDCK (C). UIC2 bound to Pgp was detected by a fluorescent secondary antibody and analyzed by flow cytometry. Pictures from a typical experiment were shown. Normal IgG2a was used as a negative control.

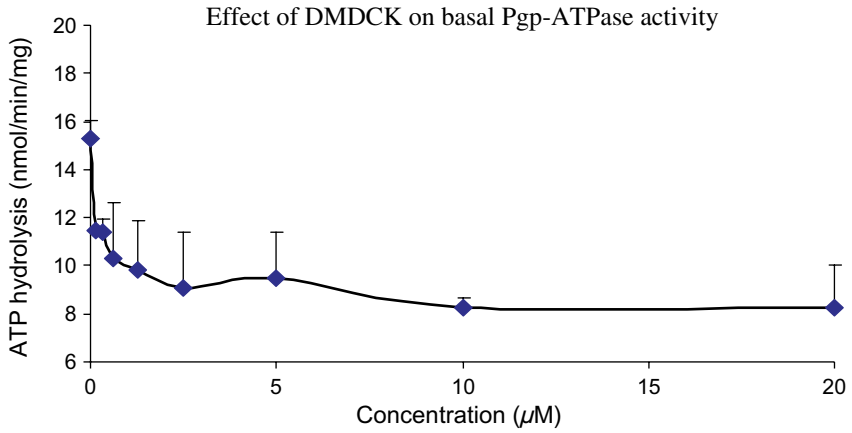

Figure 6. Effects of DMDCK on basal Pgp-ATPase activity. Pgy-rich membrane vesicles were prepared from Pgp-overexpressing K562/Dox cells. Pgp-ATPase activity was measured with other major membrane ATPases suppressed.

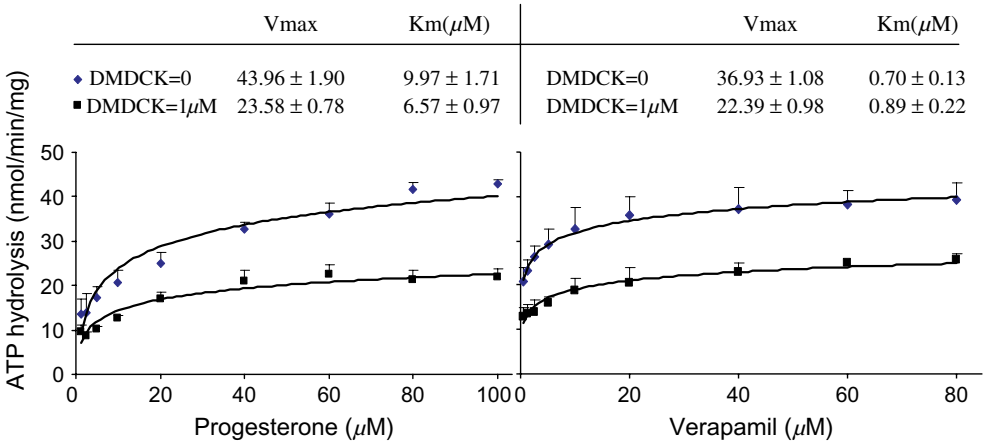

Figure 7. Effects of DMDCK on substrate-stimulated Pgp-ATPase activity. ATP hydrolysis rate was measured in the presence of various concentrations of progesterone (left panel) or verapamil (right panel) in the absence (♦) or presence (■) of 1 μM DMDCK. Values were means ± SD of three experiments and basal activity was subtracted as background before curve fitting.

increases Pgp-MDR reversing activity, whereas 4-methoxy alone slightly reduces the activity. It can be speculated that DMDCK might bind to substrate site(s) of Pgp but cannot be transported and consequently it inhibits transportation and ATP hydrolysis. DMDCK exhibits much higher Pgp-MDR reversing activity and relatively lower cytotoxicity and thus is potentially a good Pgp modulator. Further molecular and in vivo experiments are warranted.

4. Experimental

4.1. General

Doxorubicin, vinblastine, puromycin, paclitaxel, verapamil, Hoechst 33342, rhodamine 123 (Rh-123), sulforhodamine B (SRB), 3-(4,5-dimethylthiazol-2-yl)-2,5-diphenyl tetrazolium bromide (MTT), MgATP, and other reagent grade chemicals were purchased from Sigma/Aldrich Co. (St. Louis, MO, USA). Cell culture media and supplements were products of Gibco-BRL (MD, USA). Nitrocellulose membranes and secondary antibody (horseradish-peroxidase-conjugated anti-rabbit IgG) were from Bio-Rad (CA, USA), and the anti-Pgp antibody was from Calbiochem (La Jolla, USA). Anti-MDR1 monoclonal UIC2 (UIC2 mouse monoclonal anti-human MDR1) was from Immunotech (PA, USA). Goat anti-mouse IgG2a-PE and normal IgG2a were from Santa Cruz Biotechnology (CA, USA). Nuclear magnetic resonance spectra (NMR) were recorded on a Varian NMR-300 MHz spectrometer in $CDCl_3$. Optical rotations were measured on a PE343 polarimeter. Mass spectra (MS) were carried out on a Thermo-Finnigan LCQ Advantage mass spectrometer.

4.2. Preparation of DMDCK and MMDCK

The intermediate (±)-*cis*-khellactone was obtained through basic hydrolysis of PA as described previously.[19] Subsequently, 3,4-dimethoxycinnamic acid (310 mg, 1.5 mmol) was added to a mixture of (±)-*cis*-khellactone (80 mg, 0.31 mmol), dichloromethane (5 mL), *N*,*N*′-dicyclohexylcarbodiimide (206 mg, 1 mmol), and 4-dimethylaminopyridine (4 mg, 0.032 mmol). The mixture was stirred/refluxed for 3 h,

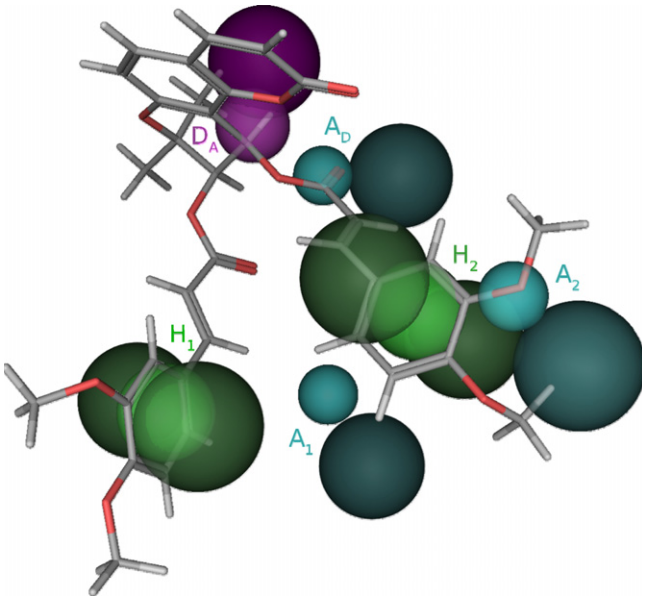

Figure 8. Enantiomer B of DMDCK docked into the general pharmacophore pattern of drugs at the verapamil binding site of Pgp[17]. H_1 and H_2 are aromatic regions. The smaller brighter green sphere corresponds to center of the aromatic ring and the darker green spheres corresponds to the directional features of the aromatic rings. A_1, A_2, and A_D are HB acceptor points. The smaller cyan sphere corresponds to the location of the acceptor atoms and the bigger to the direction of the hydrogen bond. D_A is a HB donor point (magenta spheres).

cooled to room temperature, filtered, and the filtrate was separated and purified by repeated flash silica gel 60 column chromatograph (petroleum ether/EtOAc, 4:1). Fractions were monitored by LC/MS and purified DMDCK (22 mg, 11% yield) was obtained. Same treatment with 4-methoxycinnamic acid (270 mg, 1.5 mmol) provided MMDCK (17 mg, 7% yield).

DMDCK appeared to be white amorphous solid with a zero specific rotation. ^{1}H NMR δ ppm ($CDCl_3$): 6.20 (1H, d, J = 9.5 Hz, 3-H), 7.60 (1H, d, J = 9.5 Hz, 4-H), 7.38 (1H, d, J = 8.6 Hz, 5-H), 6.85 (1H, d, J = 8.6 Hz, 6-H), 1.56 and 1.46 (3H each, s, 2′-(CH_3)$_2$), 5.52 (1H, d, J = 5.0 Hz, 3′-H), 6.97 (1H, d, J = 5.0 Hz, 4′-H), 6.98 and 6.97 (1H each, s, 2× (Ar-2-H)), 6.76 (2H, d, J = 8.1 Hz, 2× (Ar-5-H)), 6.95 (2H, d, J = 8.1 Hz, 2× (Ar-6-H)), 3.88, 3.86, 3.80, and 3.77 (3H each, s, 4× (OCH_3)), 6.31 (2H, d, J = 15.8 Hz, 2× (Ar-CH=)), 7.60 (2H, d, J = 15.8 Hz, 2 × (–OCOCH=)). MS (ESI) for $C_{36}H_{34}O_{11}$: 665 $[M+Na]^+$. The compound was identified to be (±)-3′,4′-bis(3,4-dimethoxycinnamoyl)-*cis*-khellactone.

MMDCK appeared to be white amorphous solid with a zero specific rotation. ^{1}H NMR δ ppm ($CDCl_3$): 6.21 (1H, d, J = 9.6 Hz, 3-H), 7.59 (1H, d, J = 9.6 Hz, 4-H), 7.38 (1H, d, J = 8.6 Hz, 5-H), 6.85 (1H, d, J = 8.6 Hz, 6-H), 1.56 and 1.46 (3H each, s, 2′-(CH_3)$_2$), 5.52 (1H, d, J = 5.0 Hz, 3′-H), 6.76 (1H, d, J = 5.0 Hz, 4′-H), 7.40, 7.38 (2H each, d, J = 7.9 Hz, 2× (Ar-2-H, Ar-6-H)), 6.84 and 6.82 (2H each, d, J = 7.9 Hz, 2× (Ar-3-H, Ar-5-H)), 3.82, 3.81 (3H each, s, OCH_3), 6.33 (2H, d, J = 15.9 Hz, 2× (Ar-CH=)), 7.63 (2H, d, J = 15.9 Hz, 2× (–OCOCH=)). MS (ESI) for $C_{34}H_{30}O_9$: 605 $[M+Na]^+$. The compound was identified as (±)-3′,4′-bis(4-methoxycinnamoyloxy)-*cis*-khellactone.

4.3. Cell lines and cell culture

Human hepatoma cell line HepG2 and its doxorubicin-selected Pgp-overexpressing subline HepG2/Dox,[23] human leukemia cell line K562 (ATCC No. CCL-243) and its doxorubicin-selected Pgp-overexpressing subline K562/Dox[24] were grown in RPMI 1640 medium containing 10% FBS and 100 U antibiotics. Human epidermoid carcinoma cell line KB-3-1 and its vinblastine-selected Pgp-overexpressing subline KB V1[25] were grown in MEM containing 10% FBS and 100 U antibiotics, at 37 °C in a humidified 5% CO_2 incubator. Five hundred nanograms per milliliter of vinblastine, 1.2 μM doxorubicin, and 0.1 μM doxorubicin were added separately into medium of KB V1 cell, HepG2/Dox cell, and K562/Dox cell to maintain the MDR phenotype. All MDR cells were grown in drug free medium for at least 7 days before test.

4.4. Growth inhibitory and MDR reversal assays

Cell growth inhibitory effects of various drugs were determined by SRB assay in KB-3-1, KB V1, HepG2, and HepG2/Dox cells. MTT cytotoxicity assay was performed in K562 and K562/Dox cells. Growth inhibition by a drug was evaluated by IC_{50} (concentration of a drug causing a 50% inhibition of cell growth) as described previously.[19] Each growth inhibition experiment was repeated at least three times and results were expressed as means ± standard deviation (SD). Solvents and media were included as blank control. MDR reversing activity of a drug was evaluated by comparing IC_{50} values of an anticancer drug in the presence and absence of a test compound. Medium control was subtracted as background and verapamil, a Pgp substrate and competitive inhibitor, was used as the positive control.

4.5. Drug efflux assay

Rh-123 retention assay was performed as described previously with minor modifications.[7] Briefly, 1×10^6 cells in 1 mL complete growth medium were incubated with 5 μg/mL Rh-123 at 37 °C for 1 h to allow Rh-123 uptake. Rh-123 loaded cells were washed with ice-cold PBS twice, and resuspended in fresh medium containing the test compound. After 1 h of incubation at 37 °C, cells were washed with ice-cold PBS twice and resuspended in 1 mL ice-cold PBS. Fluorescence of cellular Rh-123 was analyzed by flow cytometry. Verapamil was included as a positive control.

Hoechst 33342 efflux assay was performed in a 96-well format. Each well was seeded with 5×10^4 HepG2/Dox cells in 100 μl medium and incubated overnight. The medium was replaced with 100 μl fresh medium containing 20 μg/mL Hoechst 33342 and cells were incubated at 37 °C for 1 h. Cells were washed with 100 μl ice-cold PBS twice and 100 μl fresh medium containing a test

Table 4. Possible orientations identified by pharmacophore search with verapamil-based template

	H_1	H_2	A_1	A_2	A_D
DMDCK (A)					
	Phenyl R_2	Phenyl R_1		*m*-Methoxy R_2	Ester C=O R_1
	Phenyl R_2	Phenyl R_1	Ester C=O R_2	*m*-Methoxy R_1	
	Phenyl R_1	Phenyl R_2		*p*-Methoxy R_2	
	Phenyl R_2	Phenyl R_1		*m*-Methoxy R_1	
	Coumarin	Phenyl R_1		*p*-Methoxy R_1	
	Coumarin	Phenyl R_1		*m*-Methoxy R_1	
	Coumarin	Phenyl R_2		*p*-Methoxy R_2	
	Coumarin	Phenyl R_2		*m*-Methoxy R_2	
	Coumarin	Phenyl R_2	Coumarin C=O		
	Phenyl R_1	Phenyl R_2			Ester C=O R_2
	Phenyl R_1	Phenyl R_2		*m*-Methoxy R_2	
	Phenyl R_2	Coumarin	Ester C=O R_2		
	Phenyl R_2	Phenyl R_1			Ester C=O R_1
	Phenyl R_2	Phenyl R_1		*p*-Methoxy R_1	
	Phenyl R_2	Phenyl R_1	Ester C=O R_2		
DMDCK (B)					
	Phenyl R_1	Phenyl R_2		*m*-Methoxy R_2	Ester C=O R_2
	Phenyl R_1	Phenyl R_2	Ester C=O R_1	*m*-Methoxy R_2	
	Phenyl R_2	Phenyl R_1		*p*-Methoxy R_1	Ester C=O R_1
	Phenyl R_2	Coumarin	Ester C=O R_2		
	Coumarin	Phenyl R_2			Ester C=O R_1
	Coumarin	Phenyl R_1		*p*-Methoxy R_1	
	Coumarin	Phenyl R_1	Coumarin C=O		
	Coumarin	Phenyl R_2		*m*-Methoxy R_2	
	Coumarin	Phenyl R_2	Ester C=O R_2		
	Coumarin	Phenyl R_2	Coumarin C=O		
	Phenyl R_1	Coumarin	Coumarin C=O		
	Phenyl R_1	Phenyl R_2			Ester C=O R_2
	Phenyl R_1	Phenyl R_2		*m*-Methoxy R_2	
	Phenyl R_1	Phenyl R_2		*p*-Methoxy R_2	
	Phenyl R_1	Phenyl R_2	Ester C=O R_1		
	Coumarin	Phenyl R_2	Ester C=O R_1		
	Phenyl R_2	Phenyl R_1		*m*-Methoxy R_1	
	Phenyl R_2	Phenyl R_1	Ester C=O R_1		
MMDCK (A)					
	Phenyl R_2	Phenyl R_1	Ester C=O R_2	*m*-Methoxy R_1	
	Phenyl R_2	Phenyl R_1		*p*-Methoxy R_1	
	Coumarin	Phenyl R_2		*p*-Methoxy R_2	
	Phenyl R_1	Phenyl R_2		*p*-Methoxy R_2	
	Phenyl R_2	Coumarin	Ester C=O R_2		
	Phenyl R_2	Phenyl R_1			Ester C=O R_1
	Phenyl R_2	Phenyl R_1	Ester C=O R_2		
MMDCK (B)					
	Phenyl R_2	Coumarin	Ester C=O R_2		
	Coumarin	Phenyl R_1		*p*-Methoxy R_1	
	Coumarin	Phenyl R_2		*p*-Methoxy R_2	
	Coumarin	Phenyl R_2	Ester C=O R_2		
	Phenyl R_1	Phenyl R_2			Ester C=O R_2
	Phenyl R_1	Phenyl R_2		*p*-Methoxy R_2	
	Phenyl R_1	Phenyl R_2	Ester C=O R_1		
	Phenyl R_2	Phenyl R_1			Ester C=O R_1
	Phenyl R_2	Phenyl R_1		*p*-Methoxy R_1	
DCK (A)					
	Phenyl R_2	Coumarin	Ester C=O R_2		
DCK (B)					
	Phenyl R_2	Coumarin	Ester C=O R_2		
	Coumarin	Phenyl R_1			Ester C=O R_1
	Coumarin	Phenyl R_2	Ester C=O R_2		
	Phenyl R_1	Phenyl R_2			Ester C=O R_2
	Phenyl R_2	Coumarin			Ester C=O R_1

H_1 and H_2: hydrophobic points (aromatic rings) of the template.
A_1, A_2, and A_D: HB accepter points of the template.
A and B: the two enantiomers of pyranocoumarin.
R_1 and R_2 represent the two side chains on C-3′ and C-4′ of pyranocoumarin (see Fig. 1).

drug was added. After incubation at 37 °C for 1 h, cells were washed with ice-cold PBS twice and cellular fluorescence of Hoechst 33342 was measured at λ_{ex} = 365 nm and λ_{em} = 460 nm by a BMG FLUOstar OPTIMA Microplate Reader.

4.6. Western blot analysis of Pgp expression

HepG2/Dox, K562/Dox and KB V1 cells were treated with 4, 8 or 20 μM DMDCK in cell growth medium for 72 h. Cells were harvested, lysed, and centrifuged as described previously.[19] Supernatants were collected and protein concentration was determined by Bradford assay. Samples containing 50 μg protein were subjected to 10% SDS–PAGE and electro-transferred to nitrocellulose membranes that were blocked with 3% non-fat milk/0.1% Tween 20/TBS, 100 mM NaCl in 10 mM Tris, pH 7.5, incubated with anti-Pgp antibody for 1 h at room temperature followed by horseradish-peroxidase-conjugated secondary antibody for another 1 h at room temperature. Protein bands were detected by the ECL method. KB-3-1, K562, and HepG2 extracts were also studied as a basal expression level control.

4.7. Pgp-rich membrane vesicle preparation and Pgp-ATPase activity assay

Pgp-enriched membrane vesicles were prepared from Pgp-overexpressing K5652/Dox cells. Pgp-ATPase activity was assayed based on phosphate-release catalyzed by the membrane vesicle with all other major membrane ATPases inhibited.[19] Base line controls contained 100 μM Na_3VO_4, pH 10.0, and/or ethanol (vehicle) at a maximum final concentration of 2% v/v. All experiments were repeated three times.

4.8. UIC2 reactivity assay

Pgp reactivity with the conformation-sensitive monoclonal antibody UIC2 was performed as described previously.[19] Cytofluorimetric analysis was performed on a FACSCalibur flow cytometer. Normal mouse IgG_{2a} served as a negative control.

4.9. Pharmacophore search with verapamil-template

GASP and SYBYL molecular modeling software were used. The fitting or docking of different conformers of DCK, DMDCK, or MMDCK onto the verapamil-based pharmacophore templates for Pgp substrates and/or inhibitors was performed in a rigid manner. During this procedure different conformers of each compound were fitted onto the pharmacophore template. In order to cover with these conformers the whole or nearly the whole conformational space of each compound, separate conformational search was performed for each compound. DCK, DMDCK, and MMDCK were racemites consisting of equal amount of dextrorotatory and levorotatory enantiomers. In this approach they were generated as **A** and **B** isomers and treated separately.

The pharmacophore model of the verapamil binding site[17] was transferred into a MOE[26] pharmacophore query using the PCHD scheme containing directional features. For all compounds extensive stochastic conformational search was performed in MOE. To better cover the conformational space the energy cutoff difference between the conformers was set to 20 kcal/mol and the failure limit to generate a new conformation increased to 200. The conformation and iteration limit stayed unchanged at 10,000. As DCK, DMDCK, and MMDCK were racemates consisting of equal amounts of dextrorotatory and levorotatory enantiomers, both isomers **A** and **B** were generated and treated separately.

The resulting conformations were then docked rigid onto the pharmacophore query allowing partial match and requiring different numbers of fitted features, starting with all 14 features and reducing the number of required features to 10 and 8. The aromatic features and their interaction sites were set as essential and hydrogen bonding as optional.

In an analog way the pharmacophore of the Hoechst binding site[18] was adopted to MOE and used as pharmacophore query. The pharmacophore search with three aromatic regions and a hydrogen acceptor set as required resulted in no matches.

Acknowledgments

We thank Mr. Lai Hau-Yun for NMR measurement. We also thank Prof. Wei Xiao-Yi in South China Botanical Garden, Chinese Academy of Sciences for optical rotation measurement.

References and notes

1. Gottesman, M. M.; Fojo, T.; Bates, S. E. Multidrug resistance in cancer: role of ATP-dependent transporters. *Nat. Rev. Cancer* **2002**, *2*, 48–58.
2. Choi, C. H. ABC transporters as multidrug resistance mechanisms and the development of chemosensitizers for their reversal. *Cancer Cell Int.* **2005**, *5*, 30.
3. Krishna, R.; Mayer, L. D. Multidrug resistance (MDR) in cancer. Mechanisms, reversal using modulators of MDR and the role of MDR modulators in influencing the pharmacokinetics of anticancer drugs. *Eur. J. Pharm. Sci.* **2000**, *11*, 265–283.
4. Tsuruo, T.; Iida, H.; Tsukagoshi, S.; Sakurai, Y. Overcoming of vincristine resistance in P388 leukemia *in vivo* and *in vitro* through enhanced cytotoxicity of vincristine and vinblastine by verapamil. *Cancer Res.* **1981**, *41*, 1967–1972.
5. Tsuruo, T.; Iida, H.; Tsukagoshi, S.; Sakurai, Y. Increased accumulation of vincristine and adriamycin in drug resistant P388 tumor cells following incubation with calcium antagonists and calmodulin inhibitors. *Cancer Res.* **1982**, *42*, 4730–4733.
6. Kukl, J. S.; Sikic, B. I.; Blume, K. G.; Chao, N. J. Use of etoposide in combination with cyclosporine for purging multidrug resistant leukemic cells from bone marrow in a mouse model. *Exp. Hematol.* **1992**, *20*, 1048–1054.
7. Wang, C.; Zhang, J. X.; Shen, X. L.; Wan, C. K.; Tse, A. K.; Fong, W. F. Reversal of P-glycoprotein-mediated

multidrug resistance by Alisol B 23-acetate *Biochem. Pharmacol.* **2004**, *68*, 843–855.
8. Martin, C.; Berridge, G.; Mistry, P.; Higgins, C.; Charlton, P.; Callaghan, R. The molecular interaction of the high affinity reversal agent XR9576 with P-glycoprotein. *Br. J. Pharmacol.* **1999**, *128*, 403–411.
9. Mistry, P.; Stewart, A. J.; Dangerfield, W.; Okiji, S.; Liddle, C.; Bootle, D.; Plumb, J. A.; Templeton, D.; Charlton, P. In vitro and in vivo reversal of P-glycoprotein-mediated multidrug resistance by a novel potent modulator, XR9576. *Cancer Res.* **2001**, *61*, 749–758.
10. Maki, N.; Hafkemeyer, P.; Dey, S. Allosteric modulation of human P-glycoprotein. Inhibition of transport by preventing substrate translocation and dissociation. *J. Biol. Chem.* **2003**, *278*, 18132–18139.
11. Anuchapreeda, S.; Leechanachai, P.; Smith, M. M.; Ambudkar, S. V.; Limtrakul, P. N. Modulation of P-glycoprotein expression and function by curcumin in multidrug-resistant human KB cells. *Biochem. Pharmacol.* **2002**, *64*, 573–582.
12. Wu, J. Y.; Fong, W. F.; Zhang, J. X.; Leung, C. H.; Kwong, H. L.; Yang, M. S.; Li, D.; Cheung, H. Y. Reversal of multidrug resistance in cancer cells by pyranocoumarins isolated from *Radix peucedani*. *Eur. J. Pharmacol.* **2003**, *473*, 9–17.
13. Martin, C.; Berridge, G.; Higgins, C. F.; Mistry, P.; Charlton, P.; Callaghan, R. Communication between multiple drug binding sites on P-glycoprotein. *Mol. Pharmacol.* **2000**, *58*, 624–632.
14. Cianchetta, G.; Singleton, R. W.; Zhang, M.; Wildgose, M.; Giesing, D.; Fravolini, A.; Cruciani, G.; Vaz, R. J. A pharmacophore hypothesis for P-glycoprotein substrate recognition using GRIND-Based 3D-QSAR. *J. Med. Chem.* **2005**, *48*, 2927–2935.
15. Ekins, S.; Kim, R. B.; Leake, B. F.; Dantzig, A. H.; Schuetz, E. G.; Lan, L.; Yasuda, K.; Shepard, R. L.; Winter, M. A.; Schuetz, J. D.; Wikel, J. H.; Wrighton, S. A. Application of three-dimensional quantitative structure–activity relationship of P-glycoprotein inhibitors and substrates. *Mol. Pharmacol.* **2002**, *61*, 974–981.
16. Seelig, A. A general pattern for substrate recognition by P-glycoprotein. *Eur. J. Biochem.* **1998**, *251*, 252–261.
17. Pajeva, I. K.; Wiese, M. Pharmacophore model of drugs involved in P-glycoprotein multidrug resistance: explanation of structural variety (hypothesis). *J. Med. Chem.* **2002**, *45*, 5671–5686.
18. Pajeva, I. K.; Globisch, C.; Wiese, M. Structure–function relationships of multidrug resistance P-glycoprotein. *J. Med. Chem.* **2004**, *47*, 2523–2533.
19. Shen, X. L.; Chen, G. Y.; Zhu, G. Y.; Fong, W. F. (±)-3′-*O*,4′-*O*-dicynnamoyl-*cis*-khellactone, a derivative of (±)-praeruptorin A, reverses P-glycoprotein mediated multidrug resistance in cancer cells. *Bioorg. Med. Chem.* **2006**, *14*, 7138–7145.
20. Shapiro, A. B.; Ling, V. Positively cooperative sites for drug transport by P-glycoprotein with distinct drug specificities. *Eur. J. Biochem.* **1997**, *250*, 130–137.
21. Mechetner, E. B.; Schott, B.; Morse, B. S.; Stein, W. D.; Druley, T.; Davis, K. A.; Tsuruo, T.; Roninson, I. B. P-glycoprotein function involves conformational transitions detectable by differential immunoreactivity. *Proc. Natl. Acad. Sci. U.S.A.* **1997**, *94*, 12908–12913.
22. Nagy, H.; Goda, K.; Arceci, R.; Cianfriglia, M.; Mechetner, E.; Szabo, G., Jr. P-Glycoprotein conformational changes detected by antibody competition. *Eur. J. Biochem.* **2001**, *268*, 2416.
23. Chan, J. Y.; Chu, A. C.; Fung, K. P. Inhibition of P-glycoprotein expression and reversal of drug resistance of human hepatoma HepG2 cells by multidrug resistance gene (mdr1) antisense RNA. *Life Sci.* **2000**, *67*, 2117–2124.
24. Le Gal, J.-M.; Morjani, H.; Manfait, M. Ultrastructural appraisal of the multidrug resistance in K562 and LR73 Cell lines from Fourier transform infrared spectroscopy1. *Cancer Res.* **1993**, *53*, 3681–3686.
25. Shen, D. W.; Cardarelli, C.; Hwang, J.; Cornwell, M.; Richert, N.; Ishii, S.; Pastas, I.; Gottesman, M. M. Multiple drug-resistant human KB carcinoma cells independently selected from high-level resistance to colchicines, doxorubicin, or vinblastine show changes in expression of specific proteins. *J. Biol. Chem.* **1986**, *261*, 7762–7770.
26. MOE 2006.08 (Molecular Operating Environment), Chemical Computing Group, 1010 Sherbrooke Street West, Suite 910; Montreal, Que., Canada H3A 2R7.